MOLEKUL
www.jmolekul.com

Articles
https://doi.org/10.20884/1.jm.2020.15.3.600

Ni/Al Layered Double Hydroxide Intercalated with Keggin Ion $[\alpha\text{-}SiW_{12}O_{40}]^{4-}$ for Iron(II) Removal in Aqueous Solution

Aldes Lesbani[1,2,3]*, Normah[1], Neza Rahayu Palapa[3], Tarmizi Taher[2], Roy Andreas[4], Risfidian Mohadi[1,2]

[1]Department of Chemistry, Faculty of Mathematics and Natural Sciences, Universitas Sriwijaya, 30662, Indonesia
[2]Research Center of Inorganic Materials and Coordination Complexes, Faculty of Mathematics and Natural Sciences, Universitas Sriwijaya, Palembang 30662, Indonesia
[3]Graduate School of Mathematics and Natural Sciences, Faculty of Mathematics and Natural Sciences, Universitas Sriwijaya, Palembang 30662, Indonesia
[4]Departement of Chemistry, Faculty of Mathematics and Natural Sciences, Universitas Jenderal Soedirman, Purwokerto 53123, Indonesia

*Corresponding author email: aldeslesbani@pps.unsri.ac.id

Received November 21, 2019; **Accepted** July 02, 2020; **Available online** November 20, 2020

ABSTRACT. Layered double hydroxide (LDH) Ni/Al-NO_3 was synthesized using a coprecipitation method under base condition following with intercalation using Keggin ion $[\alpha\text{-}SiW_{12}O_{40}]^{4-}$ to form Ni/Al-$[\alpha\text{-}SiW_{12}O_{40}]$ LDH. The LDHs were characterized using XRD, FTIR, BET, and pH_{pzc} analyses. Furthermore, LDHs were applied as adsorbent of iron(II) from aqueous solution. The adsorption process was studied through the effect of adsorption time, the concentration of iron(II), and temperature adsorption. The results show the interlayer distance of LDHs was increased from 7.408 Å to 10.533 Å after intercalation process. The adsorption of iron(II) on LDHs showed that adsorption of iron(II) on both LDHs follows pseudo first-order kinetic model with R^2 value is close to one. The adsorption process was spontaneous, with adsorption capacity up to 36.496 mg g^{-1}.

Keywords: layered double hydroxide, Ni/Al, Keggin ion, adsorption, iron(II)

INTRODUCTION

Water pollution from heavy metals has directly affected to ecological balance and also flora, fauna, and human health. The heavy metal wastewaters are produced from industrial applications such as electroplating process, smelting, metallurgical, and chemical processes. Therefore, the removal of heavy metal from wastewaters is crucial for environmental security and human health (Koju, Song, Wang, Hu, & Colombo, 2018). Various methods have been applied to remove heavy metal ions from a solution such as ion exchange, membrane filtration, coagulation, and adsorption (Taher, Mohadi, & Lesbani, 2018a). Among these methods, adsorption is an excellent method due to fast process, simple operation, low cost, and efficient removal (Imron, Said, & Lesbani, 2017). The efficiency process of adsorption depends on kinds of the adsorbent for the removal of heavy metals.

The wide range adsorbents have been used to remove heavy metal ions such as chitosan (Fan et al., 2018), cellulose (Fakhre & Ibrahim, 2018), zeolite (Qiu et al., 2018), bentonite, montmorillonite, and layered double hydroxide materials (Palapa, Mohadi, & Lesbani, 2018). Layered double hydroxide (LDH) is inorganic layer materials consists of divalent M^{2+} and trivalent M^{3+} metal ions. There is a small anion between the layer depending on synthetic conditions such as sulfate, nitrate, carbonate, or chloride (Machado, Alves de Freitas, & Wypych, 2019). The general formula of LDH is $[M^{2+}_{1-x}M^{3+}_{x}(OH)_2]^{x+}(An^-)_{x/n}]nH_2O$ with M^{2+}/M^{3+} is divalent and trivalent metal ions and An^- is interlayer anions with valence n. LDH has a positive charge net, and that charge is balanced with an anion, which is located on interlayer LDH (Carmelj, Ruengkajorn, Buffet, & O'hare, 2019). The unique properties anion on interlayer LDH can be exchanged with other anions to obtain specific properties of LDH using large anions such as complex compounds, heteropoly and isopolyoxometalate (Omwoma, Chen, Tsunashima, & Song, 2014).

The use of LDH as adsorbent of heavy metal ions has been tested by many researchers and have limitation such as low adsorbed capacity due to formation of aggregates which restrict its use widely. Thus, LDH should be improved to enhance the adsorption capacity. A new modified hydrotalcite-like

adsorbent FeMnMg-LDH has been applied as a potential material for the remediation of heavy metal contamination, such as Pb^{2+}. Mg-Fe LDH hollow nanosphere, which was prepared by one step thermal method, was used as adsorbent of heavy metal ions such as As^{5+} and Cr^{6+} with maximum adsorption capacity 176.6 mg g^{-1} for arsenic and 148.7 mg g^{-1} for chromium (Mubarak et al., 2018). Hierarchical porous Ni/Co LDH thermalization was applied an adsorbent of Cr(VI) ion with adsorption capacity 99.9 mg g^{-1} at 30 °C (Hu et al., 2019). The complex compound of $Fe(CN)_6^{4-}$ was used as intercalant of Mg-Al LDH. These materials were applied as strip test detection of heavy metal ions (Wang, Sun, Fan, & Ai, 2016). Polyoxometalate $[PW_{10}Mo_2O_{40}]^{5-}$ was used as intercalant on Zn-Al LDH and this material was characterized using X-ray diffraction, infrared spectroscopy, and cyclic voltammetry (Bi, Xu, Xu, & Liu, 2011). On the other hand, Taher et al. (2019 a,b) was used Keggin type polyoxometalate $[\alpha\text{-}SiW_{12}O_{40}]^{4-}$ as intercalant of Ca/Al LDH. Intercalated Ca/Al-$[\alpha\text{-}SiW_{12}O_{40}]$ has the ability as adsorbent of cadmium(II) and iron(II) from aqueous solution. The advantages of polyoxometalates as intercalant of LDH are that cluster compounds have various oxidation states, structures and shapes, stable, enhancing adsorption capacity, increasing basal scpacing, increase the surface area and also easy to synthesize (Lesbani & Mohadi, 2014). Thus, research intercalation of polyoxometalate onto LDH is intriguing material chemistry research until this decade.

In this research, polyoxomatalate $[\alpha\text{-}SiW_{12}O_{40}]^{4-}$ was used as intercalant of Ni/Al-NO_3 LDH to form Ni/Al-$[\alpha\text{-}SiW_{12}O_{40}]$. Materials Ni/Al-$NO_3$ LDH and Ni/Al-$[\alpha\text{-}SiW_{12}O_{40}]$ were used as adsorbent of iron(II) from aqueous solution. Iron usually found in ground water and presents in iron(II) ion with high concentration (Zhang, Zhao, Jiang, Shan, & Lu, 2014). According Indonesian standard as drinking water (MCLs) for iron is 0.3 mg/L (Indonesian Minister of Health No.492/MENKES/PER/IV/2010). Therefore, it becomes necessary to remove iron(II) from wastewater by an appropriate methods before its releasing them into the environment. According to He, Qiu, , Hu, & Liu (2018) the modified LDH which containing polyoxometalate can be remove iron(II) from wastewater. The better adsorption efficiency should be obtained by adjusting ratio of metal ions in the laminates ranges $1<n<4$, the ratio of metal ions is large, resulting in a large aperture size. However, according to Han, Lu, Wei, Wang, & Duan, (2008), the interlayer anion of LDH can be enhancing ability for removal metal ion. Furthermore, the adsorption was studied through the investigation effect of adsorption time, the concentration of iron(II), and temperature adsorption. Then kinetic and thermodynamic parameters have been obtained to explain adsorption phenomena on LDH.

EXPERIMENTAL SECTION

Chemical and Instrumentations

Chemicals are supplied from Merck and Sigma Aldrich, such as nickel(II) nitrate, aluminum(III) nitrate, iron(II) chloride, sodium hydroxide, sodium carbonate, sodium tungstate, sodium metasilicate, and, hydrochloric acid. Water was obtained from the water purification system containing Purite® ion exchange material. Characterization using X-ray powder analysis was conducted using XRD Rigaku Miniflex-600. The sample was scanned at 1 deg min^{-1}. Analysis using FTIR spectrophotometer was conducted using Shimadzu FTIR Prestige-21 using KBr Pellet and sample was recorded at wavenumber 400-4000 cm^{-1}. Determination of surface area analysis was conducted using adsorption-desorption Quantachrome apparatus at 77 K. Iron(II) was analyzed using UV-Vis spectrophotometer BioBase BK-UV 1800 PC spectrophotometer after complexation with 1,10-phenanthroline at wavelength 510 nm. Determination of pH pzc was conducted under acid-base condition using hydrochloric acid or sodium hydroxide in sodium chloride solution (Umh & Kim, 2014). Keggin ion of $K_4[\alpha\text{-}SiW_{12}O_{40}]$ was synthesized according to previously reported literature (Lesbani, Kawamoto, Uchida, & Mizuno, 2008).

Synthesis of Ni/Al-NO_3 LDH and Preparation of Ni/Al-$[\alpha\text{-}SiW_{12}O_{40}]$

Synthesis of Ni/Al-NO_3 LDH was conducted using the coprecipitation method at pH 10. Nickel(II) nitrate 0.3 M was mixed with aluminum(III) nitrate 0.1 M with an equal amount, and the mixture was constantly stirred. Sodium carbonate 0.3 M was added into the mix with the same amount of nickel-aluminum. The reaction was performed at 80 °C for 17 hours under nitrogen flows. The pH was adjusted at pH 10 using the addition of sodium hydroxide 2 M. The solid green material was formed after 17 hours' reaction time. Green materials were washed several times with water and dried at 120 °C for 48 hours to form Ni/Al-NO_3 LDH (Li et al., 2010).

Preparation of Ni/Al-$[\alpha\text{-}SiW_{12}O_{40}]$ was conducted using an ion-exchange method. One-gram Ni/Al-NO_3 LDH in water was mixed with eight grams of $K_4[\alpha\text{-}SiW_{12}O_{40}]$. The reaction was performed under atmospheric nitrogen conditions for 24 hours. Material Ni/Al-$[\alpha\text{-}SiW_{12}O_{40}]$ was obtained and washed with water. Characterization of Ni/Al-NO_3 LDH and Ni/Al-$[\alpha\text{-}SiW_{12}O_{40}]$ was carried out using XRD, FTIR, BET, and pH pzc analyses.

Adsorption Studies

Adsorption was conducted using a small reactor batch system as similarly report by Taher, Rohendi, Mohadi, & Lesbani (2018b). The adsorption process was investigated by the effect of time, the effect of iron(II) concentration, and the effect of temperature. The influence of adsorption time was studied using

various time of adsorption at 10, 20, 30, 50, 70, 90, 110, 120, 150, and 180 minutes. The effect of iron(II) concentration was studied at 10, 15, 20, 25, and 30 mg L^{-1}. The effect of temperature adsorption was studied at 303, 313, 323, and 333 K. The final concentration of iron(II) was analyzed using UV-Vis spectrophotometer after complexation with 1,10-phenanthroline at 510 nm.

RESULTS AND DISCUSSION

Figure 1 shows XRD powder patterns of Ni/Al-NO_3 LDH (a) and Ni/Al-[α-$SiW_{12}O_{40}$] (b). Material Ni/Al-NO_3 LDH has unique diffraction at 11° (003), 24° (006), 35° (009), 40° (118), and 62° (110) as similarly report by JCPDS (No.15-0087). The well-ordered layer material of Ni/Al-NO_3 was identified at 11° (003), 24° (006), and 62° (110) (Zhang et al., 2019). Intercalation of Ni/Al-NO_3 LDH with K_4[α-$SiW_{12}O_{40}$] to form Ni/Al-[α-$SiW_{12}O_{40}$] resulting XRD as shown in **Figure 1b**. The main diffraction at (003) was shifted to a lower diffraction peak at 9° (003) due to the insertion of large anion onto interlayer distance. However, the reflection of (003) appeared in two diffractions at 9° and 11° denotes anion [α-$SiW_{12}O_{40}]^{4-}$ might not be fully intercalated in interlayer, the impregnated has appeared. Similarly reported by Rives, Carriazo, and Cristina (2020) the macro-intercalant of LDH might not be successfully intercalated due to intercalation process which depends of LDH's matrix, pH and other treatments. Thao, Trung, & Van Long (2016) has been conducted Mg/Al LDH intercalated molybdate using starting treatments before intercalation process i.e., pre-swelling on solid LDHs and keep pH around 6.5. Other peaks were similar to Ni/Al-NO_3 LDH before intercalation. The interlayer distance at (003) before intercalation was 7.048 Å and after intercalation was 10.533 Å. Thus, intercalation of Keggin ion [α-$SiW_{12}O_{40}]^{4-}$ onto interlayer distance of Ni/Al-NO^3 was successfully conducted. Kulandaivalu, Azman & Sulaiman (2020) was reported that the basal spacing of reflection (110) defines the unit cell which reflecting the distance between the two metal cations within the layers. The splitting peaks between (110) and (113) also defines the presents of anion in interlayer, usually this indicated the macro-anion (Han et al., 2008).

The FTIR spectra of Ni/Al-NO_3 and Ni/Al-[α-$SiW_{12}O_{40}$] LDHs were shown in **Figure 2**. The vibration of Ni/Al-NO_3 mainly contains three parts i.e., a vibration of nitrate (1600 cm^{-1}) and carbonate (1400 cm^{-1}) as ions on interlayer, a vibration of metal (670 cm^{-1}, 810 cm^{-1}), and vibration of water molecules (3400 cm^{-1}) (Gu, Huang, Wang, Yuan, and Ding, 2019). The intensity vibration of carbonate was very sharp before intercalation. The vibration of carbonate after intercalation was largely decreased due to the exchange ion process of carbonate to Keggin ion. The wavenumber at the range 900-1100 cm^{-1} was also appeared due to the vibration of Keggin ion (νW=O, νW-O-W, νW-O-W, and νSi-O).

The nitrogen adsorption-desorption on Ni/Al-NO_3 and Ni/Al-[α-$SiW_{12}O_{40}$] LDHs is shown in **Figure 3**. There is an H3 hysteresis loop on Ni/Al-NO_3 and Ni/Al-[α-$SiW_{12}O_{40}$] LDHs with type IV isotherm curve. Materials were classifying as mesoporous materials (Kong & Adidharma, 2019). The BET analysis, as shown in **Table 1**, has largely increased of the surface area of Ni/Al-NO_3 to Ni/Al-[α-$SiW_{12}O_{40}$], indicating the opening of an interlayer distance of LDH. The pore volume and pore diameter of materials were also increased after the intercalation process.

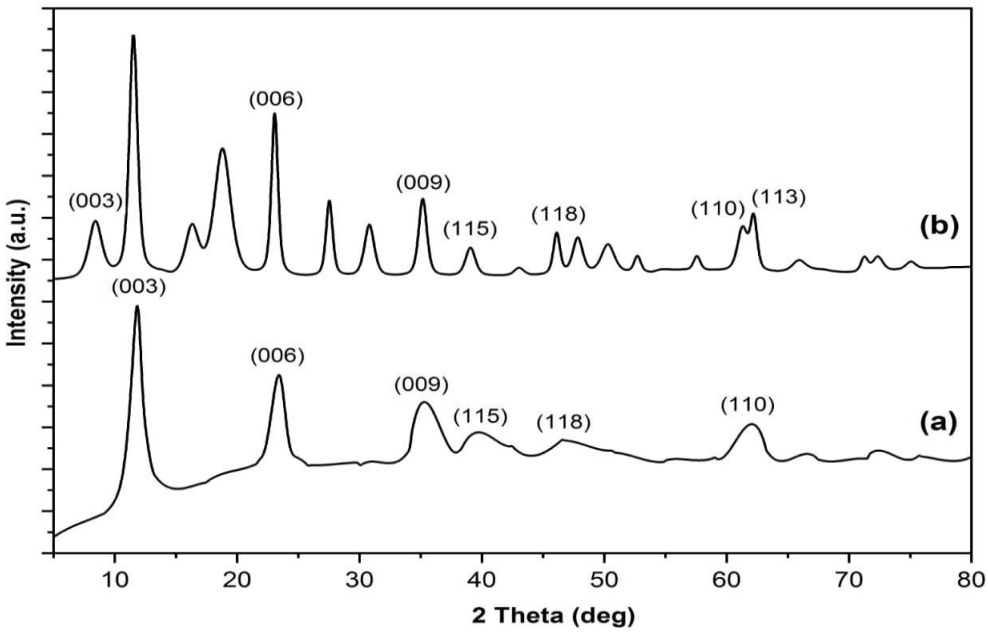

Figure 1. XRD powder patterns of Ni/Al-NO_3 (**a**) and Ni/Al-[α-$SiW_{12}O_{40}$] (**b**) LDHs

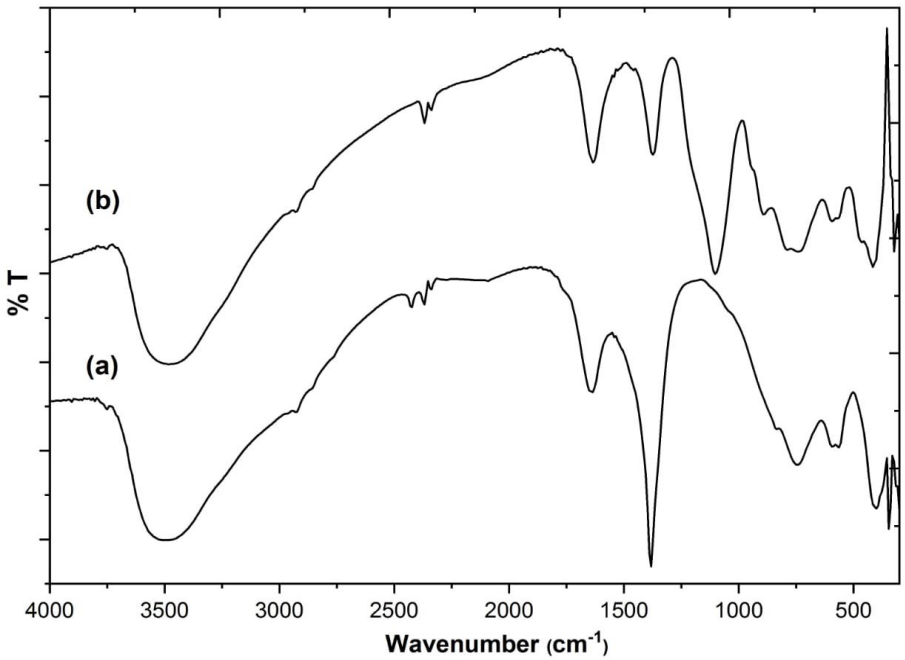

Figure 2. FTIR spectra of Ni/Al-NO_3 (**a**) and Ni/Al-[α-$SiW_{12}O_{40}$] (**b**) LDHs

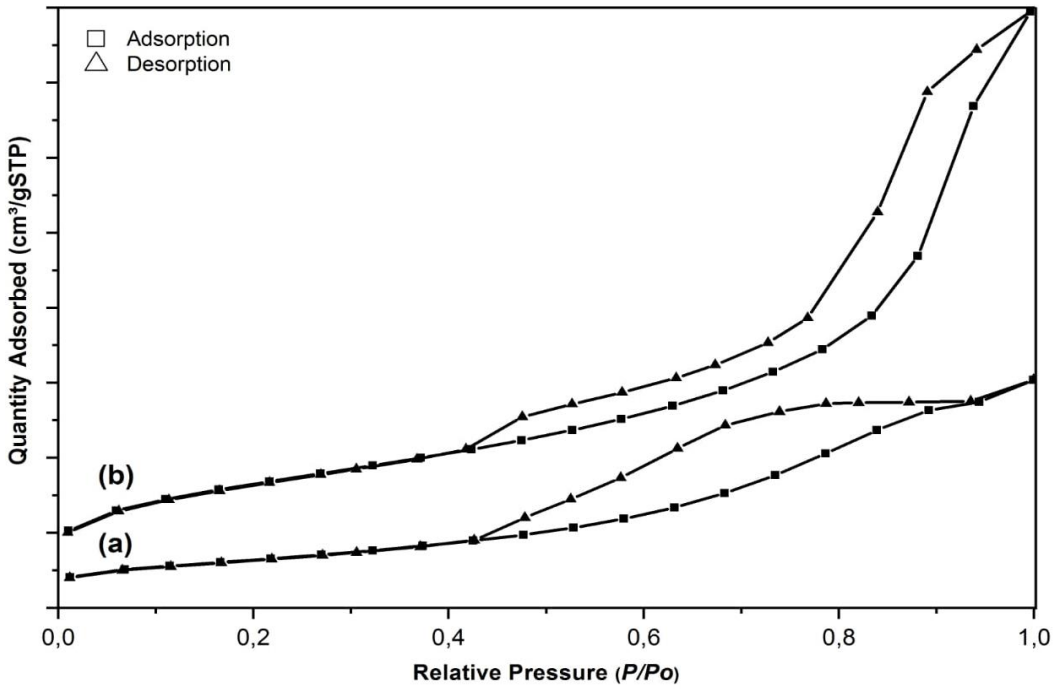

Figure 3. The BET isotherm profile of Ni/Al-NO_3 (**a**) and Ni/Al-[α-$SiW_{12}O_{40}$] (**b**) LDHs

Table 1. BET analysis of Ni/Al-NO_3 and Ni/Al-[α-$SiW_{12}O_{40}$] LDHs

Properties	LDHs	
	Ni/Al-NO_3	Ni/Al-[α-$SiW_{12}O_{40}$]
BET Surface Area (m^2 g^{-1})	58.114	116.161
Pore volume (cm^3 g^{-1}), BJH	0.118	0.237
Pore diameter (nm), BJH	7.405	9.629

The surface charges of Ni/Al-NO_3 and Ni/Al-[α-$SiW_{12}O_{40}$] LDHs were determined before materials used as adsorbent through the determination of pH_{pzc}. Both material Ni/Al-NO_3 and Ni/Al-[α-$SiW_{12}O_{40}$] have an intersection point at pH 8. The charges at that point are zero. The value below pH_{pzc} point has positive charges on the surface materials and vice versa. Thus adsorption of iron(II) on Ni/Al-NO_3 and Ni/Al-[α-$SiW_{12}O_{40}$] was conducted at pH 8.

The first process of adsorption was studied through the effect of adsorption time, as shown in **Figure 5**. The adsorption was gradually increased with increasing adsorption time and reach equilibrium at 120 minutes for both adsorbents. The kinetic pseudo first-order and pseudo second-order models were applied for data in **Figure 1** (Oktriyanti Palapa, Mohadi, & Lesbani, 2019).

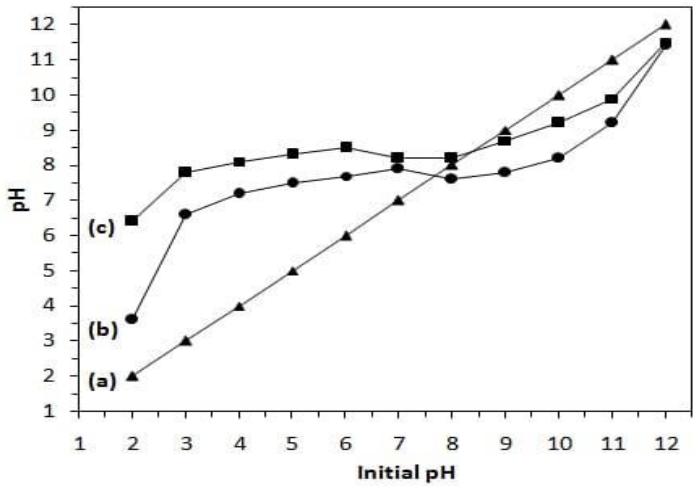

Figure 4. pH_{pzc} graph

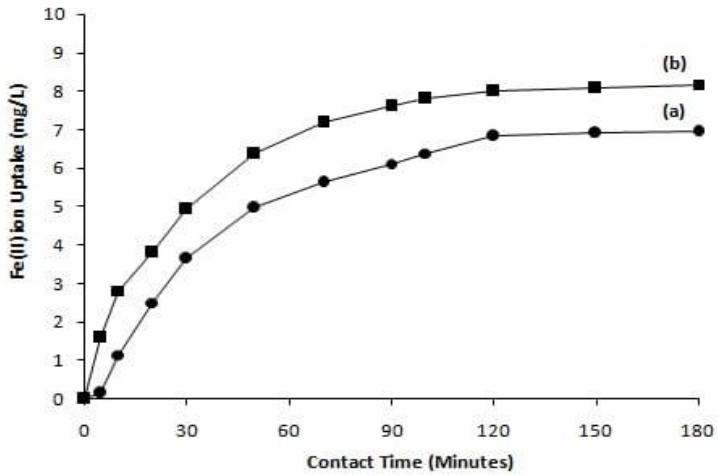

Figure 5. Effect of adsorption time of Ni/Al-NO_3 (**a**) and Ni/Al-[α-$SiW_{12}O_{40}$] (**b**) LDHs

Table 2. Kinetic Adsorption Model Ni/Al-NO_3 and Ni/Al-[α-$SiW_{12}O_{40}$]

Kinetic Adsorption Model	Kinetic Parameter	LDH	
		Ni/Al-[α-$SiW_{12}O_{40}$]	Ni/Al-NO_3
Pseudo First-Order	Qe_{Exp} (mg g^{-1})	8.178	6.947
	Qe_{Calc} (mg g^{-1})	14.385	7.881
	R^2	0.9055	0.9977
	k_1 (min^{-1})	0.0447	0.0304
Pseudo Second-Order	Qe_{Exp} (mg g^{-1})	8.178	6.947
	Qe_{Calc} (mg g^{-1})	12.919	9.099
	R^2	0.305	0.987
	k_2 (g mg min^{-1})	18.419	39.645

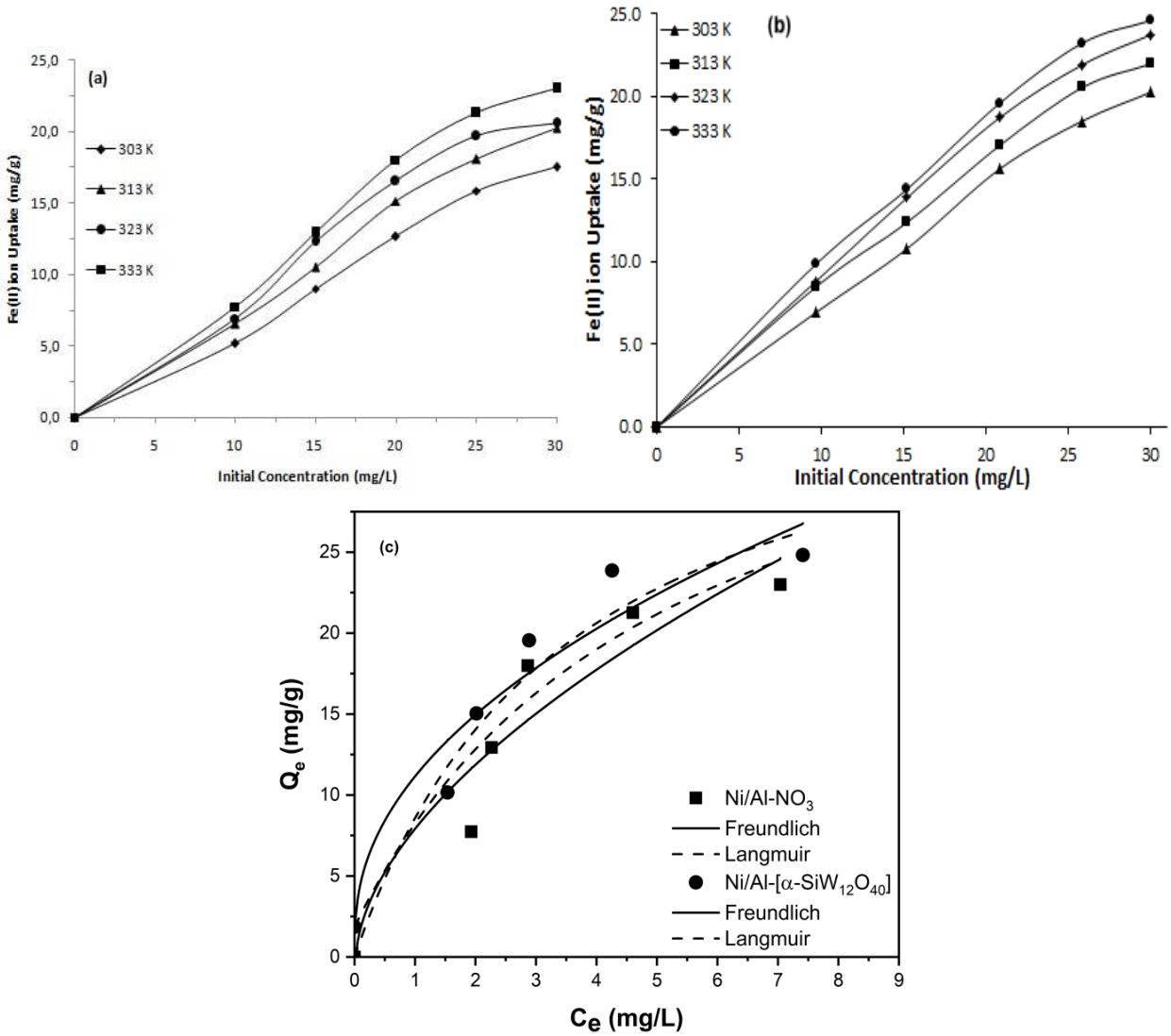

Figure 6. Effect of Concentration and temperature adsorption on Ni/Al-NO_3 (**a**), Ni/Al-[α-$SiW_{12}O_{40}$] (**b**) LDHs and isotherm adsorption (**c**)

Table 2 showed that the pseudo first-order kinetic model is appropriate for both adsorbents of Ni/Al-NO_3 and Ni/Al-[α-$SiW_{12}O_{40}$] LDHs and R^2 value is close to one. The k_1 value for Ni/Al-NO_3 and Ni/Al-[α-$SiW_{12}O_{40}$] LDHs are 0.0304 min^{-1} and 0.0447 min^{-1}, respectively indicated material Ni/Al-[α-$SiW_{12}O_{40}$] LDH has higher reactivity to adsorb iron(II) from the aqueous solution than pristine material Ni/Al-NO_3 LDH.

The effect of concentration of iron(II) and the temperature of adsorption on Ni/Al-NO_3 and Ni/Al-[α-$SiW_{12}O_{40}$] is shown in **Figure 6**. The adsorption of iron(II) was increased by increasing concentration of iron(II) and by increasing temperature adsorption. Isotherm adsorption of iron(II) was calculated using Langmuir and Freundlich adsorption isotherm model as reported by Agarwal et al. (2016) was in **Figure 6c** and **Table 3**. The Freundlich isotherm fitted the experimental data better than Langmuir isotherm model, which indicated the adsorption was multilayer coverage as shown in **Figure 6c**. **Table 3** showed that the maximum adsorption capacity was calculated by Langmuir equation obtained 60.241 mg/g for Ni/Al-NO_3 (303K) and 909.090 mg/g for Ni/Al-[α-$SiW_{12}O_{40}$] (303K). furthermore, the increasing temperature caused the adsorption capacity decreased. These findings indicated that LDH's interlayer is expanded and caused the iron molecule was difficult to adsorb. As similarly reported by Liao and Chen (2016) that the maximum adsorption capacity is favored in room temperature. Freundlich isotherm model for both LDHs is appropriate for adsorption of iron(II) on LDHs for all temperatures with R^2 value is close to one. Due to linearity R^2 of Langmuir isotherm model than adsorption capacity of iron(II) on LDHs is up to 36.496 mg g^{-1} (R^2 = 0.834).

The effect of concentration and temperature adsorption in **Figure 6** was also used to calculate the thermodynamic adsorption of iron(II) on Ni/Al-NO_3 and Ni/Al-[α-$SiW_{12}O^{40}$] LDHs. The thermodynamic data is presented in **Table 4**.

Table 3. Isotherm adsorption of iron(II) on LDH

	Isotherm	Isotherm Paramater	Temperature (K)			
			303	313	323	333
Ni/Al-NO_3	Langmuir	q_{max} (mg g^{-1})	60.241	416.670	47.393	51.282
		k_{ML} (L mg^{-1})	0.020	0.006	0.094	0.131
		R^2	0.3032	0.0216	0.4075	0.4822
	Freundlich	k_F (mg g^{-1})(L $mg)^{1/n}$	0.020	2.264	4.692	6.457
		n	0.829	0.998	1.378	1.376
		R^2	0.9626	0.9522	0.7247	0.7544
Ni/Al-[α-$SiW_{12}O_{40}$]	Langmuir	q_{max} (mg g^{-1})	909.090	77.519	51.546	36.496
		K_{ML} (L mg^{-1})	0.002	0.044	0.103	0.258
		R^2	0.002	0.422	0.806	0.834
	Freundlich	k_F (mg g^{-1})(L $mg)^{1/n}$	1.744	3.378	5.161	7.840
		n	0.947	1.149	1.324	1.630
		R^2	0.8912	0.9258	0.9441	0.8107

Table 4. Thermodynamic Parameter

	ΔG° (kJ mol^{-1})				ΔH° (kJ mol^{-1})	ΔS° (J mol^{-1} K^{-1})
	303 K	313 K	323 K	333 K		
Ni/Al-NO_3	-0.885	-1.638	-2.391	-3.144	21.927	0.075
Ni/Al-[α-$SiW_{12}O_{40}$]	-1.457	-2.028	-2.599	-3.170	15.839	0.057

The data in **Table 4** showed that adsorption of iron(II) on both Ni/Al-NO_3 and Ni/Al-[α-$SiW_{12}O^{40}$] LDHs was spontaneously processing with negative ΔG° value for all temperature conditions. The negative value of ΔS° shows to increase the randomness of the adsorption process between adsorbate iron(II) and adsorbent Ni/Al-NO_3 and Ni/Al-[α-$SiW_{12}O_{40}$] LDHs. The adsorption of iron(II) on both LDHs is categorized as physical adsorption with ΔH° value is less than 100 kJ mol^{-1}.

CONCLUSION

Material Ni/Al-NO_3 and Ni/Al-[α-$SiW_{12}O_{40}$] LDHs was successfully synthesized and used as adsorbent of iron(II) from aqueous solution. The adsorption of iron(II) on LDHs follows pseudo first-order kinetic model. The adsorption was categorized as physical adsorption with energy adsorption 15.893-21.927 kJ mol^{-1}, and adsorption capacity is up to 36.496 mg g^{-1}.

ACKNOWLEDGEMENT

The authors were thanks to Universitas Sriwijaya for supporting this research through "Hibah Profesi" to A.L at fiscal year 2019/2020 contract no. 0144.20/UN9/SB3.LP2M.PT/2019. Special thanks also to the research center of inorganic materials and coordination complexes Faculty of Mathematics and Natural Sciences for laboratory facilities for this research.

REFERENCES

Agarwal, S., Nekouei, F., Kargarzadeh, H., Nekouei, S., Tyagi, I., and Gupta. V.K. (2016). Preparation of Nickel Hydroxide Nanoplates Modified Activated Carbon for Malachite Green Removal From Solutions: Kinetic, Thermodynamic, Isotherm and Antibacterial Studies. *Process Safety and Environmental Protection*, *102*, 85-97

Bi, B., Xu, L., Xu, B., and Liu, X. (2011). Heteropoly Blue-Intercalated Layered Double Hydroxides for Cationic Dye Removal from Aqueous Solution. *Applied Clay Science*, *54*, 242-247.

Cermelj, K., Ruengkajorn, K., Buffet, J-C., and O'hare, D. (2019). Layered Double Hydroxide Nanosheet Via Solvothermal Delamination. *Journal of Energy Chemistry*, *35*, 88-94.

Fakhre, N.A., and Ibrahim, B.M. (2018). The Use of New Chemically Modified Cellulose for Heavy Metal Ion Adsorption . *Journal of Hazardous Materials. 343*, 324–331.

Fan, C., Li, K., He, Y., Wang, Y., Qian, X., and Jia, J. (2018). Evaluation of Magnetic Chitosan Beads for Adsorption of Heavy Metal Ions . *Science of the Total Environment. 627*, 1396–1403.

Gu, Z., Huang, Y., Wang, Y., Yuan, N., and Ding, J. (2019). An Aluminum Silicate Modified Ni-Al LDHs Film to Improve the Corrosion Resistance

of AZ31 Mg Alloy. *Materials Letters*, *252*, 304-307.

Han, J. B., Lu, J., Wei, M., Wang, Z. L., & Duan, X. (2008). Heterogeneous ultrathin films fabricated by alternate assembly of exfoliated layered double hydroxides and polyanion. *Chemical communications*, (41), 5188-5190.

He, X., Qiu, X., Hu, C., & Liu, Y. (2018). Treatment of heavy metal ions in wastewater using layered double hydroxides: a review. *Journal of Dispersion Science and Technology*, *39*(6), 792-801.

Hu, H., Liu, J., Xu, Z., Zhang, L., Cheng, B., and Ho, W. (2019). Hierarchical Porous Ni/Co-LDH Hollow Dodecahedron with Excellent Adsorption Property for Congo Red and Cr(VI) Ions. *Applied Surface Science*, *478* (1), 981-990.

Imron, M., Said, M., and Lesbani, A. (2017). Adsorption of Procion Red Using Layer Double Hydroxides Mg/Al. *Science and Technology Indonesia*, *2*(3), 64-67.

Koju, N.K., Song, X., Wang, Q., Hu, Z., and Colombo, C. (2018) Cadmium Removal from Simulated Groundwater Using Alumina Nanoparticles: Behaviors and Mechanisms. *Environmental Pollution, 240*, 255–266.

Kong, L., and Adidharma, H. (2019). A New Adsorption Model Based on Generalized Van der Waals Partition Function For the Description of All Types of Adsorption Isotherms. *Chemical Engineering Journal*, *375*, 122112.

Kulandaivalu, S., Azman, N. H. N., & Sulaiman, Y. (2020). Advances in Layered Double Hydroxide/Carbon Nanocomposites containing Ni 2+ and Co2+/3+ for Supercapacitors. *Frontiers in Materials*, *7*, 147.

Lesbani., A., Kawamoto, R., Uchida, S., Mizuno, N. (2008). Control of Structures and Sorption Properties of Ionic Crystals of $A_2[Cr_3O(OOCC_2H_5)_6(H_2O)_3]_2[\alpha\text{-}SiW_{12}O_{40}]$ (A = Na, K, Rb, NH_4, Cs, TMA). *Inorganic Chemistry*, *47*, 3349-3357.

Lesbani, A., and Mohadi, R. (2014). Bronsted Acid of Keggin Type Polyoxometalate Catalyzed Pinacol Rearrangement. *Bulletin of Chemical Reaction Engineering and Catalysis*, *9*(2), 136-141.

Li, K.W., Kumada, N., Yonesaki, Y., takei, T., Kinomura, N., Wang, H., and Wang, C. (2010). The pH Effects on the Formation of Ni/Al Nitrate Form Layered Double Hydroxides (LDHs) by Chemical Precipitation and Hydrothermal Method. *Materials Chemistry and Physics*, *121*, 223-229.

Liao, X. J., Chen, G. S. (2016). A hybrid hydrogel based on clay nanoplatelets and host-guest inclusion complexes. *Chinese Chemical Letters*, *27*, 583–587

Machado, J.P.E., Alves de Freitas, R., and Wypych. F. (2019). Layered Clay Minerals, Synthetic layered Double Hydroxides and Hydroxide Salts Applied as Pickering Emulsifiers. *Applied Clay Science*, *169*, 10-20.

Mubarak, M., Jeon, H., Islam, M.S., Yoon, C., Bae, J-S., Hwang, S-J., Choi, W.S., and Lee, H-J. (2018). One-Pot Synthesis of Layered Double Hydroxide Hollow Nanispheres with Ultrafast Removal Efficiency for Heavy Metal Ions and Organic Contaminants. *Chemosphere*, *201*, 676-686.

Oktriyanti, M., Palapa, N.R., Mohadi, R., and Lesbani, A. (2019). Modification of Zn-Cr Layered Double Hydroxide with Keggin ion $[SiW_{12}O_{40}]$ as Cr(VI) Adsorbent. *Indonesian Journal of Environmental Management and Sustainability*, *3*(3), 93-99.

Omwoma, S., Chen, W., Tsunashima, R., and Song, Y-F. (2014). Recent Advances on Polyoxometalates Intercalated Layered Double Hydroxides: From Synthetic Approaches to Functional Material Applications. *Coordination Chemistry Reviews*, *258-259*, 58-71.

Palapa, N.R., Mohadi, R., and Lesbani, A. (2018). Adsorption of Direct Yellow Dye from Aqueous Solution by Ni/Al and Zn/Al Layered Double Hydroxides. *AIP Conference Proceeding Series*, *2026*, 020018.

Qiu, Q., Jiang, X., Lv, G., Chen, Z., Lu, S., Ni, M., Yan, J., and Deng, X. (2018). Adsorption of Heavy Metal Ions Using Zeolite Materials of Municipal Solid Waste Incineration Fly Ash Modified by Microwave-Assisted Hydrothermal Treatment . *Powder Technology, 335*, 156–163.

Rives, V., Carriazo, D., Cristina, M. (2010). Heterogeneous Catalysis by Polyoxometalate-Intercalated Layered Double Hydroxides. *In Pillared Clays and Related Catalysts*, *978*, 321-397.

Taher, T., Mohadi, R., and Lesbani, A. (2018a). Effect of Ti4+/Clay ratio on the Properties of Titanium Pillared Bentonite and its Application for Cr(VI) Removal. *Rasayan Journal of Chemistry*, *11*(3), 1244-1254.

Taher, T., Rohendi, D., Mohadi, R., Lesbani, A. (2018b). Thermal and Acid Activation (TAA) of Bentonite as Adsorbent for Removal Methylene Blue: A Kinetics and Thermodynamic Study, *Chiang Mai Journal of Science*, *45*(4), 1770-1781.

Taher, T., Irianty, Y., Mohadi, R., Said, M., Andreas, R., and Lesbani, A. (2019a). Adsorption of Cadmium(II) using Ca/Al Layered Double Hydroxides Intercalated with Keggin Ion. *Indonesian Journal of Chemistry*, *19*(4), 873-881.

Taher, T., Christina, M.M., Said, M., Hidayati, N., Ferlinahayati., and Lesbani, A. (2019b). Removal of Iron(II) using Intercalated Ca/Al Layered Double Hydroxides with [α-$SiW_{12}O_{40}$]. *Bulletin of Chemical Reaction Engineering and Catalysis*, *14*(2), 260-267.

Thao, N. T., Trung, N. D., Van Long, D. (2016). Activity of Molybdate-Intercalated Layered Double Hydroxides in the Oxidation of Styrene with Air. *Catalysis Letters*, *146*, 918-928.

Umh, H. N., and Kim, Y. (2014). Sensitivity of nanoparticles' Stability at the Point of Zero Charge (PZC). *Journal of Industrial and Engineering Chemistry*, *20*(5), 3175-3178.

Wang, N., Sun, J., Fan, H., and Ai, S. (2016). Anion-Intercalated Layered Double Hydroxides Modified Test Strips for Detection of Heavy Metal Ions. *Talanta*, *148*, 301-307.

Zhang, L., Gong, Z., Jiang, B., Sun, Y., Chen, Z., Gao, X., and Yang, N. (2019). Ni-Al layered Double Hydroxides (LDHs) Coated SuperHydrophobic Mesh with Flower-Like Hierarchical Structure for Oil/Water Separation. *Applied Surface Science*, *490*, 145-156.

Zhang, Y., Zhao, J., Jiang, Z., Shan, D., & Lu, Y. (2014). Biosorption of Fe (II) and Mn (II) ions from aqueous solution by rice husk ash. *Biomed research international*, *2014*.